Structural Design and Control Strategy Analysis of Micro/Nano Transmission Platform

Lin Chao(林超)[1*], *Ji Jiuxiang*(纪久祥)[1], *Tao Youtao*(陶友淘)[1], *Huo Dehong*(霍德鸿)[2], *Cai Lizhong*(才立忠)[1], *Cheng Kai*(程凯)[3]

1. State Key Laboratory of Mechanical Transmission, Chongqing University, Chongqing, 400030, P. R. China;
2. School of Mechanical and Systems Engineering, Newcastle University, Newcastle Upon Tyne, NE1 7RU, UK;
3. Advanced Manufacturing and Enterprise Engineering Department, Brunel University, Uxbridge, Middlesex UB8 3PH, UK

(Received 11 March 2013; revised 20 September 2013; accepted 25 September 2013)

Abstract: A fully flexure micro/nano transmission platform (MNTP) which has five degrees of freedom is designed on the basis of bridge type amplification mechanism. According to the kinematic theory and the elastic beam theory, the theoretical output displacement equation of the platform is derived, and then piezoelectric actuator (PZT) is calibrated. Meanwhile, a full closed-loop control strategy of the platform is established using the feedforward proportional-integral-derivative (PID) compound control algorithm based on the Preisach model. Moreover, the total transfer function of the micro positioning system is derived, and the calculation method of output signal is acquired. Finally, the theoretical output displacement is verified by finite element analysis (FEA) and positioning experiments.

Key words: bridge type amplification mechanism (BTAM); micro/nano transmission platform (MNTP); piezoelectric actuator (PZT); finite element analysis (FEA); control strategies

CLC number: TH13 **Document code**: A **Article ID**: 1005-1120(2014)05-0484-08

1 Introduction

Micro/nano transmission platform (MNTP) is used to produce small linear and angular displacement. With rapid development of microelectronics technology, aerospace and biological engineering, the research of MNTP with high accuracy and stability, multiple degrees of freedom and high controllability is increasingly gaining academic attention.

So far, MNTP has become a research focus and many MNTPs have been developed in the past two decades. Zhang, et al.[1] developed a micro positioning table with long stroke. The micro positioning mechanism driven by piezoelectric actuators (PZTs) has two degrees of freedom and the displacement in X or Y directions is about 288 μm. Wang, et al.[2] proposed an MNTP based on 3-revolute-revolute-revolute (3-RRR) parallel mechanism, and successfully realized ± 70 μm displacement in both X and Y directions, as well as $\pm 0.1°$ rotation about Z axis. Zhang, et al.[3] designed a precision positioning table with three degrees of freedom, and acquired ± 300 μm displacements in Z direction and $\pm 0.25°$ rotation about both X and Y axes. Chu, et al.[4] developed a long-travel linear nano-positioning stage driven by PZTs, and 35 μm displacement along X axis was thus realized with a precision of 10 nm. Yuen, et al.[5] presented a micro positioning platform with rapid movement in X and Y directions, followed by 25 μm$\times$25 μm displacement successfully. Deepkishore, et al.[6] developed a new linkage mechanism which could achieve 18 μm displacement in X or Y direction and $\pm 1.72°$ ro-

Foundation item: Supported by the State Key Laboratory of Mechanical Transmission Independent Research Fund (SKLMT-ZZKT-2012 MS 05).

* **Corresponding author**: Lin Chao, Professor, E-mail: linchao@cqu.edu.cn.

tation around Z axis. Li, et al.[7] proposed a new type of decoupled large-displacement micro position platform with two degrees of freedom, on which the stroke of each two linear axes is 117 μm. Although the above-mentioned micro positioning platforms have high accuracy and repeatability, there still exist some disadvantages, such as small movement range. Hu, et al.[8] designed a long range nano-transmission platform based on the principle of inchworm motion. It featured a maximum linear speed of 13.9 μm/s, a minimum step of 10 nm and a movement distance of more than 20 mm. Though it met the requirements of both long displacement and high precision, it can only move along a single direction. Therefore, the study of MNTP with large displacement, high precision, and multiple degrees of freedom is challenging researchers in the field.

In addition, the control strategies are also central to the development of micro positioning platforms. Since precision can be improved by using an effective control means, the research on control algorithms and control strategies has been carried out to improve the performance of micro positioning platforms. The digital proportion integration differentiation (PID) method is widely adopted due to its effective and simple setup. Moreover, some advanced control algorithms such as fuzzy algorithm, neural network algorithm and genetic algorithm were also applied to the precision control of MNTP[9-12]. Currently, several control strategies have been used, including feedforward open-loop control, PID closed-loop control, and hybrid control which combines feedforward, closed-loop control and adaptive inverse control[13-14].

This paper presents a fully flexure MNTP with five degrees of freedom driven by PZTs. The platform adopts leaf-springs and bridge type amplification mechanism (BTAM) to realize the amplification of input displacements. Firstly, the theoretical output displacements and driving mechanism of MNTP are analyzed according to the kinematic theory and elastic beam theory. PZT actuator is calibrated. Meanwhile, the whole closed-loop control strategy of MNTP is established using the feedforward PID compound control algorithm based on the Preisach model. Moreover, the total transfer function of the positioning system is derived, and the calculation of output signal in the positioning system is performed. Finally, the finite element analysis (FEA) simulation and positioning experiments are conducted to verify the effectiveness of the control strategies.

2 Principle of Structural Design

According to the principles of machinery and compliant mechanism, the large displacement MNTP with five degrees of freedom is designed (Fig. 1), whose dimensions are 260 mm × 260 mm× 120 mm. It consists of a upper platform, a lower platform and six PZTs. The upper platform is composed of four micro displacement amplification mechanisms driven by four PZTs. And the four displacement amplifiers, symmetrically arranged, can make the upper platform to move along Z axis and rotate around both X and Y axes. The lower platform is composed of two micro displacement amplification mechanisms driven by two PZTs. It employs an asymmetric structure to realize the motion in X and Y directions. This configuration ensures the high accuracy and fast response of MNTP. MNTP is manufactured by drilling, milling, grinding, and wire electrical discharge machining (EDM), etc., on one piece of material, therefore, without gap and mechanical friction. By controlling the input voltages of the six PZTs, an MNTP with high-precision, high dynamics, and multiple degrees of freedom are obtained.

MNTP consists of 56 leaf springs and 42 rigid rods (Fig. 1), and it is fixed on an experiment table by bolts. To ensure that the piezoelectric actuator is fully engaged with the micro displacement amplification mechanism, pre-loads are applied by threaded screws. The force and motion are conveyed by the pure elastic deformation of leaf springs.

3 Performance Analysis of MNTP

Fig. 2 shows the micro-displacement amplification mechanism of MNTP. BTAM is a key com-

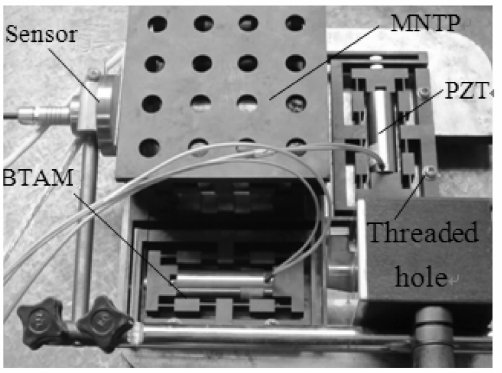

Fig. 1 MNTP with five degrees of freedom

ponent of MNTP. The input displacement of PZT is amplified by the amplification mechanism which also makes the platform move along a specified direction. Different rigid rods are connected with each other by leaf springs. In order to analyze the amplification performance of MNTP, the amplification ratio of BTAM should be first considered with the assumption that the material of different rigid rods and leaf springs is isotropic.

According to the kinematic theory and the elastic beam theory, the amplification ratio of BTAM can be expressed as

$$R_{\text{amp}} = \frac{6l_a^2 \sin 2\alpha}{t^2 \cos^4\alpha + 6l_a^2 \sin^2\alpha} \tag{1}$$

where l_a is the center distance of adjacent leaf springs, t the thickness of leaf springs, and α the amplifying angle of BTAM (Fig. 2).

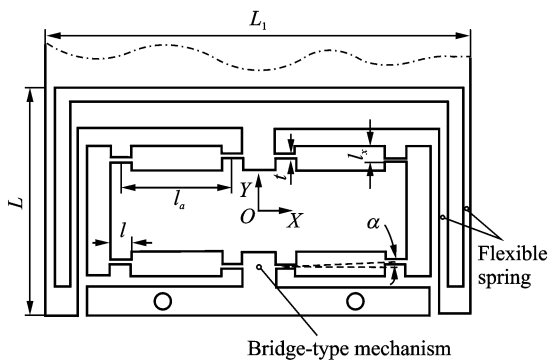

Fig. 2 Drawing of displacement amplification mechanism

Considering the relationship of geometric parameters of MNTP, the theoretical output displacements in different directions can be derived.

The linear displacements along X, Y, and Z axes can be described by the equation

$$\Delta x = \Delta y = \Delta z = \Delta L \cdot R_{\text{amp}} \tag{2}$$

The rotation angle around X or Y axis can be expressed as

$$\Delta\theta_X = \Delta\theta_Y = \arcsin\left(\frac{R_{\text{amp}} \cdot \Delta L}{L}\right) \tag{3}$$

where ΔL is the elongation displacement of PZT under variable force, which can be obtained as

$$\Delta L = \Delta L_0 \cdot \left(\frac{k_{\text{PZT}}}{k_{\text{PZT}} + k_s}\right) \tag{4}$$

where ΔL_0 is the elongation displacement of PZT under free condition, k_{PZT} the stiffness of PZT, and k_s the stiffness of MNTP.

Based on the elastic beam theory, the stiffness of the leaf spring can be determined by the equation

$$k_j = \frac{E \cdot b \cdot t^3}{12 \cdot l} \tag{5}$$

According to Eq. (5) and the principle of virtual work, the stiffness of BTAM can be calculated

$$k_g = \frac{E \cdot b \cdot t^2 \cdot (\cos\alpha)^2}{6 \cdot l^3} \tag{6}$$

From Eqs. (5,6), the stiffness of MNTP can be expressed as

$$\boldsymbol{K}_s = \begin{bmatrix} \frac{Eb[3L^2t^3(\cos\alpha)^2 + l^2t^3]}{36L^2l^3} & 0 & 0 & 0 & 0 \\ 0 & \frac{Eb[3L^3t^3(\cos\alpha)^2 + l^2t^3]}{36L^2l^3} & 0 & 0 & 0 \\ 0 & 0 & \frac{Ebt^3(\cos\alpha)^2}{8l^3} & 0 & 0 \\ 0 & 0 & 0 & \frac{Ebt^3L_1^2(\cos\alpha)^2}{16l^3} & 0 \\ 0 & 0 & 0 & 0 & \frac{Ebt^3L_1^2(\cos\alpha)^2}{16l^3} \end{bmatrix} \tag{7}$$

where t, α, l, L and L_1 are the structural parameters of the displacement amplification mechanism in Fig. 2, b the thickness of BTAM, and E the Young's modulus.

Substituting Eq. (7) into Eq. (4), ΔL is obtained. Then according to Eqs. (2,3), the displacements along X, Y and Z axes can thus be determined.

4 Drive and Control Strategies

4.1 Drive mechanism of MNTP

PZT is usually adopted as the actuator of micro positioning system. It works by utilizing the inverse piezoelectric effect, which means when an electric field is applied on PZT, it will generate a small deformation, accompanied by the micro-displacement of MNTP. The inverse piezoelectric effect of PZT can be expressed as follows

$$S = x^{E} \cdot T' + d_{33} \cdot E \tag{8}$$

where d_{33} is the piezoelectric constant, S the strain, T' the stress, E the electric field strength, and x^{E} the elastic constant.

For accurate and reliable positioning of MNTP, PZT used in the experiments has been calibrated under a free loading condition. By varying input displacements for PZT (model 40VS15), the output displacement values are collected by a capacitance displacement sensor (model Micro-Epsilon CS5). The calibration tests are repeated three times and the average values measured in the tests are shown in Fig. 3.

From Fig. 3, it can be concluded that there is slight deviation between actual output displacements and target displacements. The overall errors are within 0.1 μm range mainly due to the effect of the electromechanical coupling. The effect makes PZT exhibit hysteresis, creep, and nonlinear, etc., which are the main factors that generate errors. Therefore, a well-calibrated PZT can also help to improve the control accuracy of MNTP.

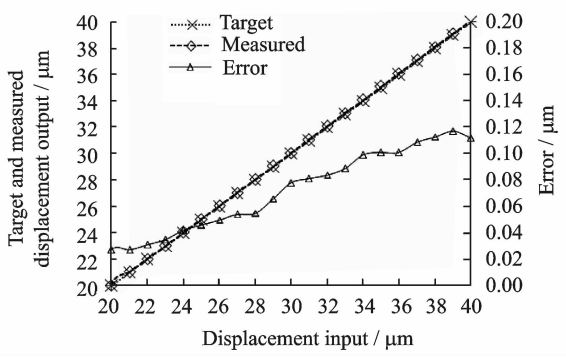

Fig. 3 Calibration test results

4.2 Control strategies of MNTP

To effectively eliminate the displacement difference of PZT, the encapsulated ceramic with strain gauge sensor (SGS) is utilized. In addition, in order to reduce the stiffness of MNTP and obtain larger motion distance and swing angles, the lower platform adopts the aforementioned asymmetric structure. But the asymmetric structure will increase the coupled displacement and affect the platform precision. A full closed-loop control system is thus designed to improve the positioning performance of the platform. Fig. 4 presents the schematic of the positioning system and Fig. 5 the block diagram of the basic control algorithm. The main control process can be expressed as follows: first, the driving control signal $R_i(kT)$ is sent out by computer, and then the feedforward controller based on the Preisach model predicts the output values $U_d(kT)$ more accurately by a certain control voltage sequence. Meanwhile, by a D/A converter, high voltages are generated to drive PZT, which will make the platform have an extremely small displacement $C(s)$. The micro displacement can be measured by capacitance displacement sensors. And the position voltage signal $x(kT)$ is sent back to the computer by the A/D converter, then the signal $x(kT)$ will compare it with the signal $R_i(kT)$ to obtain the deviation signal $e(kT)$. By the PID controller, a certain offset $\Delta U(kT)$ will be generated to compensate the hysteresis and creep effects of the piezoelectric ceramic as well as external disturbances, so as to realize precise positioning.

Taking the movement in X direction as an example, the differential equation of the positioning system holds

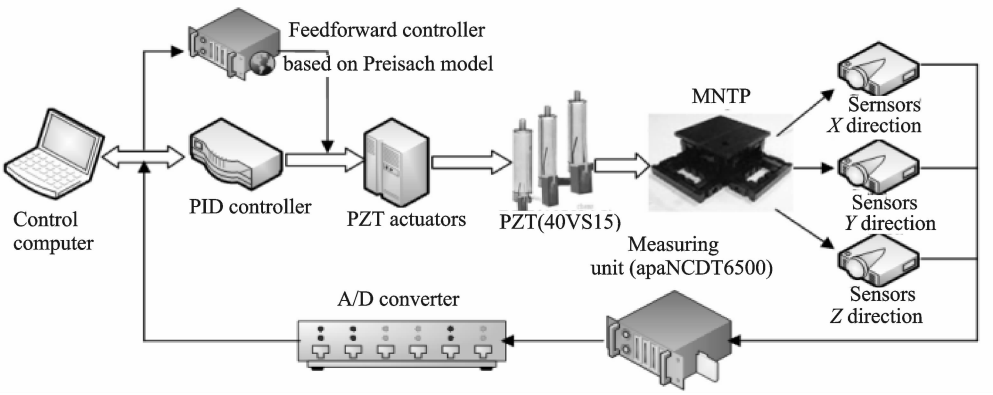

Fig. 4 Full closed-loop control principle of positioning system

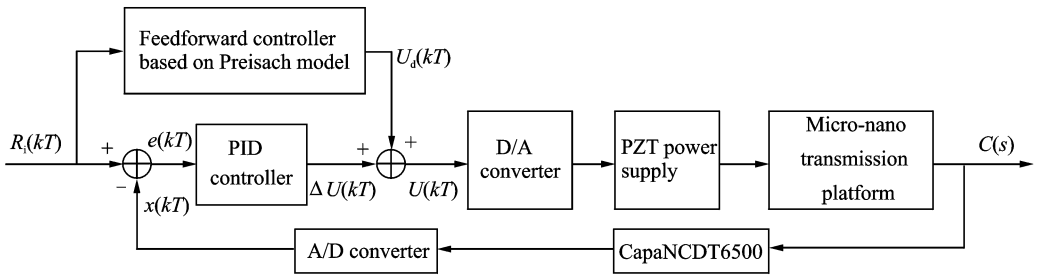

Fig. 5 Feedforward PID control algorithm based on Preisach model

$$m\frac{\mathrm{d}^2x}{\mathrm{d}t^2}+\mu\frac{\mathrm{d}x}{\mathrm{d}t}+(k_{\mathrm{PZT}}+k_{\mathrm{s}})x=$$

$$k_{\mathrm{PZT}}\cdot\Delta L\left(1-\frac{k_{\mathrm{PZT}}}{k_{\mathrm{PZT}}+k_{\mathrm{g}}}\right) \tag{9}$$

where m is the mass of MNTP, μ the damping coefficient, k_{PZT} the stiffness of PZT, k_{s} the stiffness of MNTP, k_{g} the stiffness of BTAM, ΔL the elongation displacement of PZT under variable force, and x the output displacement along X direction of MNTP.

According to Eq. (9), the transfer function of the MNTP in X direction can be obtained as

$$G_X(s)=\frac{k_{\mathrm{g}}k_{\mathrm{PZT}}}{(k_{\mathrm{PZT}}+k_{\mathrm{g}})(k_{\mathrm{PZT}}+k_{\mathrm{s}})}\cdot\frac{\omega_n^2}{s^2+2\zeta\omega_n s+\omega_n^2} \tag{10}$$

where ω_n is the natural frequency of MNTP, ζ the relative damping coefficient of MNTP.

Similarly, MNTP transfer functions in Y and Z directions are introduced by the equations

$$G_Y(s)=\frac{k_{\mathrm{g}}k_{\mathrm{PZT}}}{(k_{\mathrm{PZT}}+k_{\mathrm{g}})(k_{\mathrm{PZT}}+k_{\mathrm{s}})}\cdot\frac{\omega_n^2}{s^2+2\zeta\omega_n s+\omega_n^2}$$

$$G_Z(s)=\frac{4k_{\mathrm{g}}k_{\mathrm{PZT}}}{(4k_{\mathrm{PZT}}+k_{\mathrm{g}})(4k_{\mathrm{PZT}}+k_{\mathrm{s}})}\cdot\frac{\omega_n^2}{s^2+2\zeta\omega_n s+\omega_n^2}$$

Since the output of computer is a digital signal, D/A conversion and high voltage amplification are prerequisite for PZT actuator to generate a DC high voltage, which makes MNTP accomplish precise positioning. The PZT controller here is equivalent to a scaling up link whose transfer function can be expressed by

$$G_1(s)=\gamma_v \tag{11}$$

where γ_v is the amplification coefficient of the PZT controller.

Therefore, the transfer function of the feedback system is as follows

$$G_3(s)=\frac{\Delta L}{R_{\mathrm{amp}}\cdot\Delta L}=\frac{1}{R_{\mathrm{amp}}} \tag{12}$$

Based on Eqs. (10−12), the transfer function of the positioning system moving along X direction can be expressed as

$$G(s)=\frac{G_1(S)\cdot G_X(S)}{1+G_1(S)\cdot G_X(S)\cdot G_3(S)}=$$

$$\frac{R_{\mathrm{amp}}\cdot\gamma_v\cdot k_{\mathrm{g}}\cdot k_{\mathrm{PZT}}\cdot\omega_n^2}{\gamma_v\cdot k_{\mathrm{g}}\cdot k_{\mathrm{PZT}}\cdot\omega_n^2+R_{\mathrm{amp}}\cdot(k_{\mathrm{PZT}}+k_{\mathrm{g}})\cdot(k_{\mathrm{PZT}}+k_{\mathrm{s}})\cdot(s^2+2\zeta\omega_n s+\omega_n^2)} \tag{13}$$

Similarly, the transfer function of the positioning system along Y and Z directions can be written as

$$G'(s)=\frac{G_1(S)\cdot G_Y(S)}{1+G_1(S)\cdot G_Y(S)\cdot G_3(S)}=$$

$$\frac{R_{\mathrm{amp}}\cdot\gamma_v\cdot k_{\mathrm{g}}\cdot k_{\mathrm{PZT}}\cdot\omega_n^2}{\gamma_v\cdot k_{\mathrm{g}}\cdot k_{\mathrm{PZT}}\cdot\omega_n^2+R_{\mathrm{amp}}\cdot(k_{\mathrm{PZT}}+k_{\mathrm{g}})\cdot(k_{\mathrm{PZT}}+k_{\mathrm{s}})\cdot(s^2+2\zeta\omega_n s+\omega_n^2)} \tag{14}$$

$$G''(s)=\frac{G_1(S)\cdot G_Z(S)}{1+G_1(S)\cdot G_Z(S)\cdot G_3(S)}=\frac{4R_{\text{amp}}\cdot\gamma_v\cdot k_g\cdot k_{\text{PZT}}\cdot\omega_n^2}{4\gamma_v\cdot k_g\cdot k_{\text{PZT}}\cdot\omega_n^2+R_{\text{amp}}\cdot(4k_{\text{PZT}}+k_g)\cdot(4k_{\text{PZT}}+k_s)\cdot(s^2+2\zeta\omega_n s+\omega_n^2)} \tag{15}$$

Based on Eqs. (13－15), the output of the positioning system in X, Y and Z directions can be obtained as

$$\begin{bmatrix}c(s)\\c'(s)\\c''(s)\end{bmatrix}=\begin{bmatrix}G(s)&0&0\\0&G'(s)&0\\0&0&G''(s)\end{bmatrix}\cdot\begin{bmatrix}U_d(kT)+k_pe(kT)+k_i\sum e(kT)+k_d\{e(kT)-e[(k-1)T]\}\\U_d(kT)+k_pe(kT)+k_i\sum e(kT)+k_d\{e(kT)-e[(k-1)T]\}\\U_d(kT)+k_pe(kT)+k_i\sum e(kT)+k_d\{e(kT)-e[(k-1)T]\}\end{bmatrix} \tag{16}$$

where T is the sampling period of the control system. k_p, k_i and k_d represent the proportion, integral and differential coefficients of the PID controller, respectively.

5 Simulation and Experimental Analyses

The simulation is performed by the commercial FEA package ANSYS. The FEA model and displacement contours in different directions are illustrated in Fig. 6. The platform is made of 65Si2Mn, and its mechanical properties are shown in Table 1. The structural parameters are shown in Fig. 2 and Table 2.

Table 1 Mechanical properties of 65Si2Mn

Young's modulus/GPa	Poisson's ratio	Density/(kg·m^{-3})	Yield strength/MPa
210	0.28	7 850	1 176

Table 2 Key structural parameters of MNTP

l_a/mm	l_x/mm	l/mm	L_1/mm	L/mm	t/mm	α/(°)
20	6	8	98	58	0.8	1.8

In order to validate the effectiveness of the positioning control system, the feedforward PID rcontroller based on the Preisach model is integrated into the PZT controller. The device in Fig. 7 is to implement the control principle shown in Fig. 5, and it includes PZTs (40VS15), XE-500/501 modularized PZT controller, the capacitance displacement sensor (CS5 with a measuring range

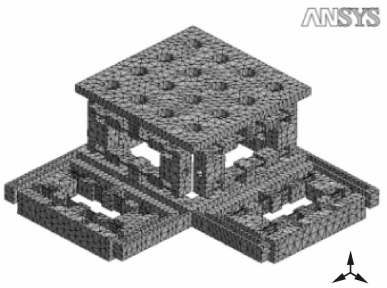

(a) Meshing of MNTP

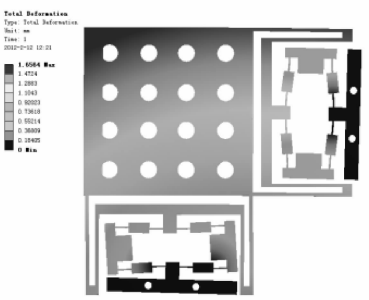

(b) Displacement in X axis direction

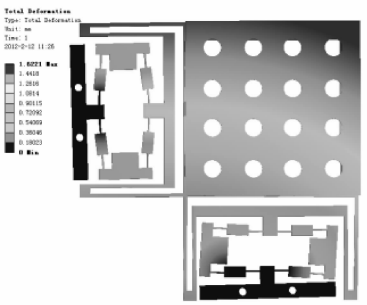

(c) Displacement in Y axis direction

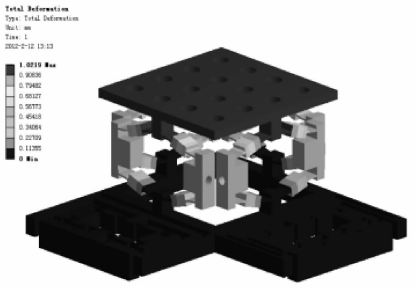

(d) Displacement in Z axis direction

Fig. 6 FEA model and movement simulation

of 5 mm and the highest resolution of 3.75 nm), a capacitance displacement sensor controller (capaNCDT6500), an RS6500 circuit controller and computers. Taking the movement in X axis direction as an example, the specific testing method is as follows: the PZT controller controls the output displacement of PZT, and then the capacitance displacement sensor collects the output displacement signals of MNTP, the signals are subsequently sent back to the computer and the PID controller so as to readjust the platform output.

For the better test results, the range of 20—40 μm is chosen as the PZT's testing output. The test results of MNTP in different directions are shown in Figs. 8(a—f).

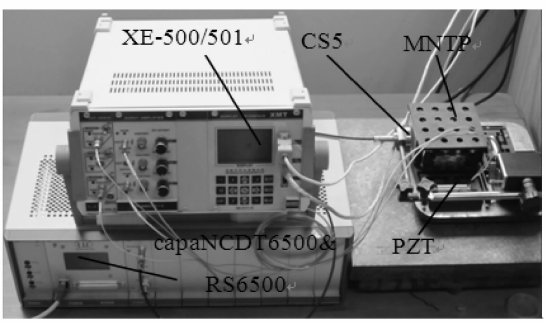

Fig. 7 Experimental apparatus for testing positioning performance

From Figs. 8(a, c, e), it can be concluded that when PZT output displacement is within 20—40 μm, the positioning system has a good repeated positioning performance, and the measured results in X, Y and Z axes directions are basically identical. It can also be known that the minimum and maximum output displacement is 117.612 μm and 355.863 μm, respectively, and the repeated positioning errors are within 6—8 μm range. In Figs. 8(b, d, f), the experimental results agree well with the theoretical results and the FEA results, which further verifies the efficiency of the PID control algorithm based on the Preisach model. Besides, the positioning errors are mainly due to the change of material properties caused by local high temperature in the wire EDM processing. The change of material properties in turn results in the variation of stiffness and the increase of processing errors. Moreover, the asymmetric structure of the lower platform can also cause the nonlinear displacement coupling errors of the platform. All of these will affect the precision of the micro positioning system. Therefore, further optimization design about the control system, structural parameters and machining method of the platform are essential to MNTP for achieving the higher precision.

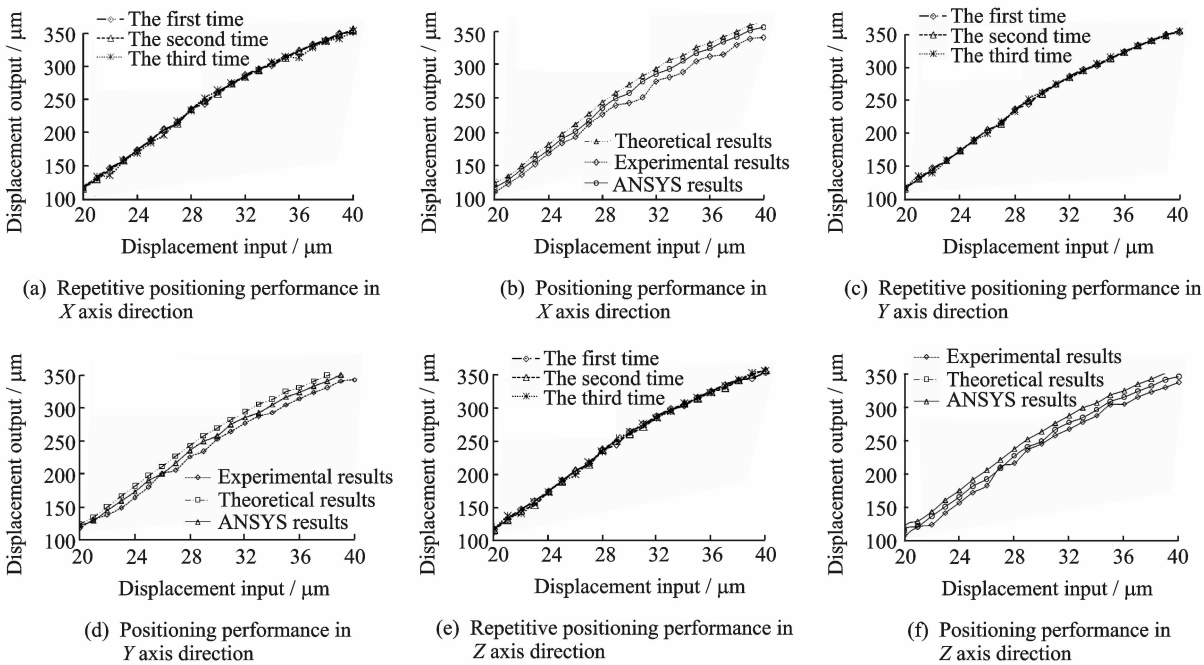

Fig. 8 Positioning performance tests in X, Y, and Z axis directions

6 Conclusions

The following conclusions can be drawn from this research:

(1) A long stroke MNTP, driven by PZT, with five degrees of freedom is designed. The amplification and guidance mechanism of micro displacement is achieved by flexure hinge. In addition, the structural design and displacement amplification performance of MNTP are analyzed.

(2) The driving mechanism of MNTP is analyzed, and the PZT actuator is calibrated. As a result, the overall positioning errors are within 0.1 μm range. Meanwhile, the full closed-loop control strategy of MNTP is established using the feedforward PID compound control algorithm based on the Preisach model. Moreover, the total transfer functions of the positioning system are derived, and the calculation method of the output signal of the positioning system is obtained.

(3) The experimental apparatus is built to assess the local performance. The maximum output displacement of the positioning system is 355.863 μm and the repetitive positioning errors are kept within 6—8 μm. Finally, the experiment results, the FEA results and the theoretical values are in good agreement. The results also further verify the effectiveness of the PID control algorithm based on the Preisach model.

References:

[1] Zhang Y F, Gong J L. Structure and parameter design for two degrees of freedom micro-positioning mechanism with large travel[J]. Journal of Mechanical Engineering, 2010, 46(23): 30-35. (in Chinese)

[2] Wang W, Hu P H, Zeng Q, et al. Theory design method of a flexure mechanism for parallel micromotion working table[J]. Metrology Test Technology & Verification, 2006, 16(6): 4-7. (in Chinese)

[3] Zhang J L, Chen W Y, Ke X R, et al. Design and simulation of a 3-DOF micro-positioning worktable [J]. Modern Manufacturing Engineering, 2009(3): 39-42. (in Chinese)

[4] Chu C L, Fan S H. A novel long-travel piezoelectric-driven linear nano-positioning stage[J]. Precision Engineering, 2005(30): 85-95. (in Chinese)

[5] Yuen K Y, Sumeet S A, Aphale S O. Design, analysis and control of a fast nano positioning stage[C]// Proceedings of the 2008 IEEE/ASME International Conference on Advanced Intelligent Mechatronics. [S. l.]:IEEE, 2008:451-456.

[6] Deepkishore M, Dong J Y, Eakkachai P W, et al. A SOI-MEMS-based 3-DOF planar parallel-kinematics nano-positioning stage[J]. Sensors and Actuators, A Physical, 2008, 147: 340-351.

[7] Li Y M, Xu Q S. Structural design and control strategy analysis of micro/nano transmission platform [J]. IEEE/ASME Transactions on Mechatronics, 2010, 15(1): 125-135.

[8] Hu C D, Zhao M R, Li Y Q, et al. Study on design and experimentation of piezoelectric micro-moving platform with nano-step and long-range[J]. Chinese Journal of Sensors and Actuators, 2009, 22(6):803-807. (in Chinese)

[9] Jie D G, Sun L N, Qu D S, et al. Fuzzy-reasoning based self-tuning PID control for piezoelectric micro-displacement system[J]. Journal of Harbin Institute of Technology, 2005, 37(2):145-147.

[10] Yong Y K, Aphale S S, Moheimani S O R. Design, identification, and control of a flexure-based XY stage for fast nanoscale positioning[J]. IEEE Transactions on Nanotechnology, 2009, 8(1):46-53.

[11] Li C, Tan Y. A hybrid neural network based modeling for hysteresis [C]// Proceedings of the 2005 IEEE International Symposium on, Mediterrean Conference on Control and Automation. Piscataway, USA: [s. n.],2005:53-58.

[12] Wai R J, Lin C M, Peng Y F. Robust CMAC neural network control for LLCC resonant driving linear piezoelectric ceramic motor[J]. IEE Proceedings: Control Theory and Applications, 2003, 150(3): 221-232.

[13] Yang C, Zhao Q, Wang H R, et al. Study on intelligent control system of two-dimensional platform based on ultra-precision positioning and large range [J]. Precision Engineering, 2010, 34: 627-633.

[14] Liaw H C, Shirinzadeh B, Smith J. Robust neural network motion tracking control of piezoelectric actuation systems for micro/nanomanipulation[J]. IEEE Transactions on Neural Networks, 2009, 20(2):356-366.

(Executive editor: Zhang Tong)